Element Transfer Behaviors of Agglomerated CaF_2-ZrO_2 Fluxes in EH36-Shipbuilding Steel Subject to High-Heat Input Submerged Arc Welding

ANGRAN CHEN[1,2], YANYUN ZHANG[1,2], THERESA COETSEE[3], IMANTS KALDRE[4],

and CONG WANG[1,2,*]

[1]Key Laboratory for Ecological Metallurgy of Multimetallic Mineral (Ministry of Education), Northeastern University, Shenyang, 110819, Liaoning, P.R. China

[2]School of Metallurgy, Northeastern University, Shenyang, 110819, Liaoning, P.R. China

[3]Department of Materials Science and Metallurgical Engineering, University of Pretoria, Pretoria, 0002, South Africa

[4]Institute of Physics, University of Latvia, Riga, 1004, Latvia

*Correspondence to Cong Wang. Email: wangc@smm.neu.edu.cn

Abstract

EH36-shipbuilding steel has been welded by CaF_2-ZrO_2 fluxes with designed ZrO_2 additions. Possible chemical and electrochemical reactions have been postulated to analyze alloying element transfer behaviors. The decomposition of ZrO_2 during SAW has been validated by applying the gas–slag–metal equilibrium model and the O supply capacity of ZrO_2 has been quantified. For the entire compositional range, O content has been controlled within a well-maintained range from 220 to 400 ppm, and the transferred quantity of Zr content reaches to the maximum value of 120 ppm. It is further demonstrated that ZrO_2 addition incurs appreciable Si loss within the weld metal.

I. Introduction

Compared with other welding techniques, submerged arc welding (SAW) has long been preferred for welding thick shipbuilding plates owing to deep penetration, high manufacturing efficiency, and low production cost.[1,2] Although higher heat input in SAW could allow enhanced deposition productivity, it may usher in deteriorated mechanical performances for the weld metal (WM), largely due to the generation of significant amount of heat within the weld pool.[3,4] Accumulated heat in the weld pool may lead to the formation of brittle and coarse-grained microstructures within the WM.[5,6] One method to address such issues is to appropriately design the flux, which could promote acicular ferrite (AF) formation, thereby enhancing the overall performance of the WM.[7,8,9]

It is acknowledged that a reasonable O content may facilitate AF formation, which is determined by the O supply capacity of the flux.[10,11,12] Chai *et al.*[11] compared the levels of

WM O content with different CaF_2-based fluxes applied for SAW and found such capacity of specific oxide could be ranked as follows: CaO, K_2O, Na_2O, TiO_2, Al_2O_3, MgO, SiO_2, and MnO (from high to low). Meanwhile, it was revealed that the addition of Zr to the EH36 steel could form Zr-O complex inclusions and enhance WM tensile strength and impact toughness.[13] Furthermore, it is pointed out that an appropriate content of ZrO_2 of 12 wt pct in the flux could optimize viscosity and surface tension, which determines thermal and electrical properties of the fluxes.[14] However, Natalie *et al.*[15] found that it was difficult to correlate flux ZrO_2 content with WM mechanical performance as ZrO_2 was expected to be amphoteric, which renders deciphering the function of ZrO_2 rather ambiguous.

It has been proven by Potapov *et al.*[16] that ZrO_2 is susceptible to dissociation in the molten pool during SAW. Bang *et al.*[17] further designed ZrO_2-bearing fluxes for SAW and pointed out that Zr could replace Si in the SiO_2 network, which could influence the transfer behavior of Si, an essential element that influences the overall performance of the WM.[7,11] However, due to complex slag-metal reactions and electrochemical reactions involved during SAW, the roles played by ZrO_2 in adjusting major alloying element contents in the WM are far from being completely understood.[18] Therefore, this work aims to analyze and quantify transfer behaviors of O, Zr, and Si with different ZrO_2 contents, potentially establishing due relationships that may bear theoretical insights for rational flux designs and desired WM properties.

II. Experimental

Within this framework, a series of specifically formulated CaF_2-ZrO_2 fluxes were employed to join EH36-shipbuilding steel.[10] Incorporation of CaF_2 is proven to reduce melting temperature and, thus, increase fluidity of involved fluxes.[19,20] Five agglomerated CaF_2-ZrO_2 fluxes with ZrO_2 contents varying from 5 to 25 wt pct were designed according to the CaF_2-ZrO_2 binary phase diagram.[21] Fluxes containing 5, 10, 15, 20, and 25 wt pct ZrO_2 were designated as F-1, F-2, F-3, F-4, and F-5, respectively. CaF_2 and ZrO_2 powders (>99 wt pct, Aladdin Co., Ltd., China) were selected as raw materials for each flux formulation. Weighed CaF_2 and ZrO_2 powders (totally 1.5 kg for each flux formulation) were mixed in a V-blender at 0.5 Hz for 1 hour to ensure homogenization. Subsequently, 0.5 kg of ammonium silicate solution (Atlantic, molar ratio 2.8, and water content 50 wt pct) was added to agglomerate the mixed powders. Afterward, agglomerated powders were passed through two screens with different sizes of 14 and 40 mesh to form small pellets. The prepared pellets were then baked at 700 °C for 3 hours to remove moisture and other possible impurities. Components of each agglomerated flux and slag were determined using X-ray fluorescence spectroscopy (XRF, ZXS Primus II, Rigaku, Japan). Chemical compositions of each flux recipe are presented in Table I.

Table I. Chemical Compositions of Fluxes (Weight Percent)

Fluxes No.	CaF_2	ZrO_2	SiO_2	Na_2O
F-1	84.28	4.88	6.81	4.02
F-2	79.6	9.66	6.74	3.98
F-3	74.81	14.26	6.79	4.13
F-4	70.14	18.87	6.93	4.05
F-5	65.32	23.91	6.76	3.99

EH36-shipbuilding steel and CHW-S3 were selected as the BM and welding wire, respectively. Bead-on-plate double-wire single-pass submerged arc welding (MZS-1250, Shandong Aotai Electric, China) was performed (DC- 850 A/32 V for electrode forward, AC-625 A/36 V for electrode backward) on the pre-polished BM. The heat input and welding speed were set at 60 kJ/cm and 500 mm/min.

As shown in Figure 1, thickness of 10 mm WM was cut in the center of the welding beads. Then, each cut WM was drilled at five different locations by using a Φ 3 drill bit, and the drill-mixed chips were used as samples to measure the metallic elemental compositions. Metallic elemental compositions in the BM, welding wire, and WM were determined using inductively coupled plasma optical emission spectrometry (Perkin Elmer Optima 8300 DV ICP-OES). C and O content measurements were conducted using a LECO analyzer (CS230 for C and ONH836 for O). Chemical compositions of the BM and wires are presented in Table II.

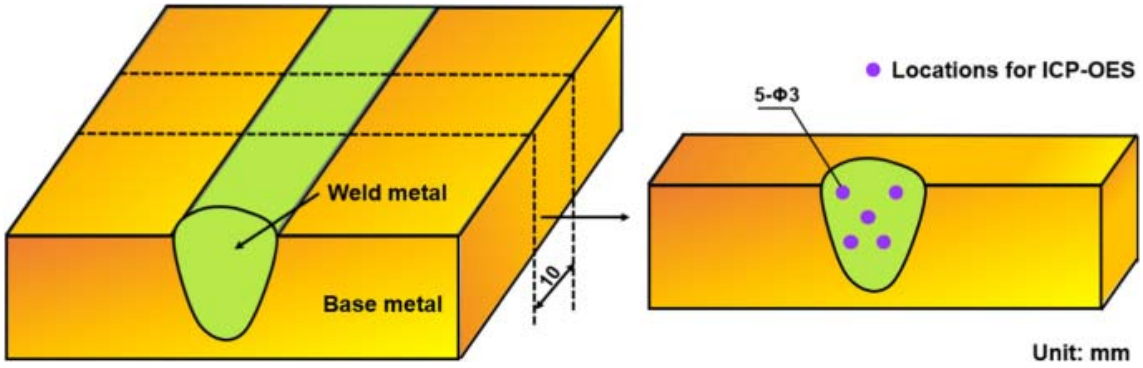

Fig. 1. Specific locations for ICP-OES

Table II. Chemical Compositions of BM and Wire (Weight Percent)

Material	C	O	Zr	Si	Mn	Ti	Al	S	Ni
BM	0.173	0.0031	0	0.150	1.53	0.009	0.034	0.010	0.018
Wire	0.135	0.0030	0	0.072	1.66	0.001	0.008	0.003	0.001

Each WM was cross sectioned and polished by automatic polishing machine (UNIPOL-1200M), followed by 4 wt pct nital solution etching. Optical stereomicroscope (SZ61, Olympus, Japan) was applied to observe the WM bead morphology to calculate the dilution value of the BM and the wire. The Equilib module in FactSage 7.3, containing FactPS, FToxid, and FSstel databases, was selected to calculate possible chemical reactions.[22] 2000 °C was selected as the equilibrium temperature for calculating ZrO_2 activity.[23]

III. Results and Discussion

Previous studies have pointed out that WM formation during the SAW process involves physical fusion of the BM and welding wire and the occurrence of a series of chemical reactions between the flux (slag) and weld pool.[11,24] Similar to the studies by Zhang *et al.*,[24] nominal content (NC), as defined by Eq. [1], has been introduced to evaluate WM composition contributed by physical dilution of the BM and the welding wire. Additionally, the determination of the transfer direction and level of a specific alloying element undergoing treatment with a designated flux component is conducted *via* the Δ value, as illustrated in Eq. [2].[24] Variations of Δ value of main alloying elements are illustrated to evaluate the effect of ZrO_2 content of the flux on the transfer of O, Zr, and Si. The δ value, as defined by Eq. [3], is introduced to determine whether the slag loses or gains specific composition after the SAW process.[24] A positive δ value implies the slag gains corresponding component, while a negative δ value reveals that this component is lost from the slag. δ values of each flux component are given in Table III to facilitate analysis for the element transfer behaviors of main elements between the slag and the weld pool.

$$\text{NC} = \text{BM composition} \times \text{BM dilution value} + \text{wire composition} \times \text{wire dilution value}, \quad (1)$$

$$\Delta \text{ value} = \text{WM determined composition} - \text{NC}, \quad (2)$$

$$\delta \text{ value} = \text{slag composition} - \text{flux composition}. \quad (3)$$

Table III. δ Values of Each Slag Composition (Weight Percent)

Fluxes No.	δCaF_2	δZrO_2	δSiO_2	δNa_2O	δMnO	δFeO
F-1	−0.94	−0.61	−0.17	−0.28	0.78	1.23
F-2	−2.04	−0.74	−0.07	−0.2	0.85	2.22
F-3	−2.02	−0.83	−0.09	−0.2	0.93	2.32
F-4	−2.84	−0.89	−0.07	−0.19	1.14	2.82
F-5	−3.42	−1.09	−0.02	−0.14	1.43	3.36

Figure 2 illustrates the nominal content, analytical content, and ΔO, as a function of the ZrO_2 content. It is shown that the nominal O content maintains a relatively low level of 30 ppm, and the analytical O content ranges from 220 to 400 ppm with ZrO_2 content addition increasing from 5 to 25 wt pct. Furthermore, ΔO content, indicated by the green column representing the difference between the analytical and the nominal O content, improves from

190 to 370 ppm. The high level of ΔO, compared to the low nominal O content for each WM, reveals that the WM primarily gains O through chemical reactions between the slag and the weld pool rather than solely through the BM and the welding wire.[24]

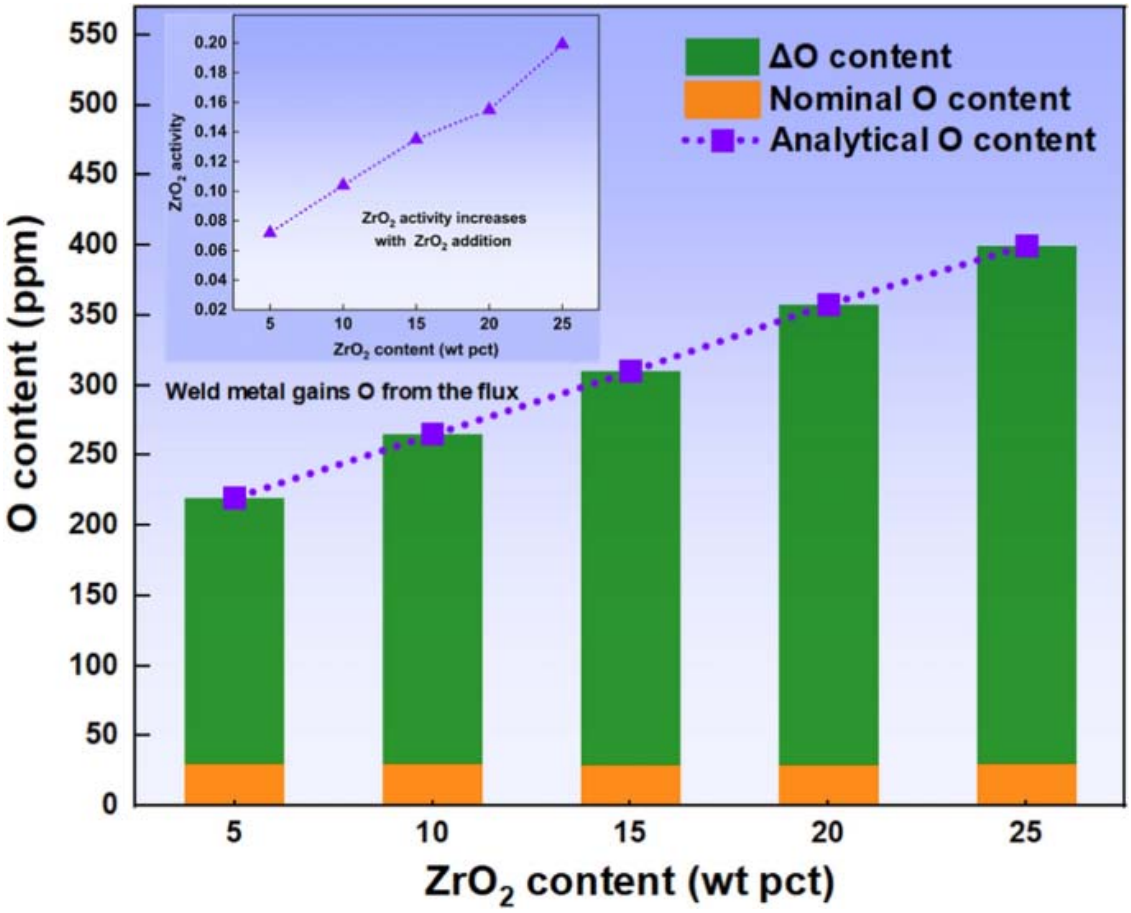

Fig. 2. WM O variation as a function of ZrO_2 content in the flux. Inset figure shows the activity of ZrO_2 in the flux at 2000 °C

It is vital to understand the slag–metal chemical reactions further to analyze the variation of the transferred O level.[24] Chai *et al.*[11] concluded that all oxides tended to decompose into suboxides and release O_2 under the arc plasma. Zhang *et al.*[24] further confirmed the decomposition of flux might release O_2 through thermodynamic calculations. Therefore, it is assumed that suboxides and O_2 may form as a result of the decomposition of ZrO_2, which primarily controls the quantity of O transfer.[24] Thermodynamic calculations using FactSage 7.3 with the gas–slag–metal model[25] confirmed the presence of ZrO and O_2 in the gaseous phases (see Table V in Appendix). Consequently, it is postulated the decomposition of ZrO_2 through Reaction [4] governs the transfer of O between the flux and the weld pool.

$$2\,(\mathrm{ZrO_2}) = 2\mathrm{ZrO}\,(\mathrm{g}) + \mathrm{O_2}\,(\mathrm{g})\,. \tag{4}$$

According to the thermodynamic calculation by FactSage 7.3 illustrated in Figure 2, the activity of ZrO_2 (2000 °C) in the flux increases from 0.07 to 0.20 with ZrO_2 level increasing from 5 to 25 wt pct. The enhanced ZrO_2 activity implies that an increased decomposition of ZrO_2

promotes the formation of O_2, and thus, the O_2 partial pressure (PO_2), which further promotes the transfer of O from the slag to the weld pool.[3,26]

It is expected the O content of the WM reflects the O supply capacity (oxygen potential) of one specific oxide in the flux.[11] Figure 3 illustrates the relationship between the WM O content (Y-axis) and different oxide contents in the flux (X-axis). As shown by the red triangles in Figure 3, it is found that the WM possesses higher O content compared to TiO_2, SiO_2, and MnO in the range of 5 to 25 wt pct ZrO_2 in the flux according to the study by Chai *et al.*.[11] Hence, ZrO_2 is further considered a significant contributor of O for SAW. Meanwhile, adding ZrO_2 to the flux within the range of 5 to 25 wt pct enables each WM to maintain O content in the range of 200 to 500 ppm, which tends to facilitate AF formation.[10]

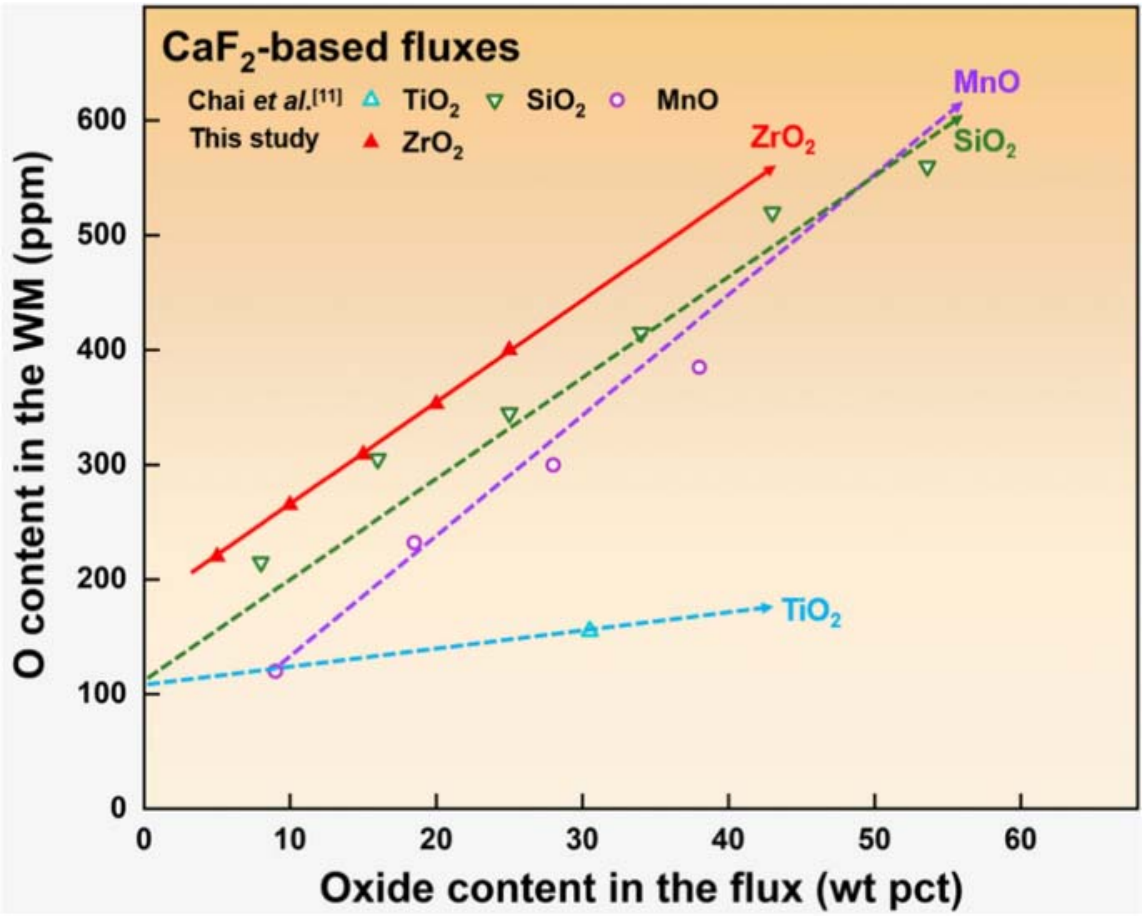

Fig. 3. WM O content as a function of different oxide contents in the flux.[11] (The figure is adapted with permission from Ref. 11)

Figure 4 presents the content of Zr transferred into the WM as a function of ZrO_2 content. It can be observed that the value of ΔZr remains positive for all WMs, which indicates substantial Zr is transferred from the slag to the weld pool. Meanwhile, thermodynamic calculations conducted using FactSage 7.3 confirm the presence of Zr and O in the weld pool (Table V, Appendix A). Therefore, it is postulated that the Zr content is dictated by Reaction [5] at the slag–metal interface.

$$(ZrO_2) = [Zr] + 2[O]. \quad (5)$$

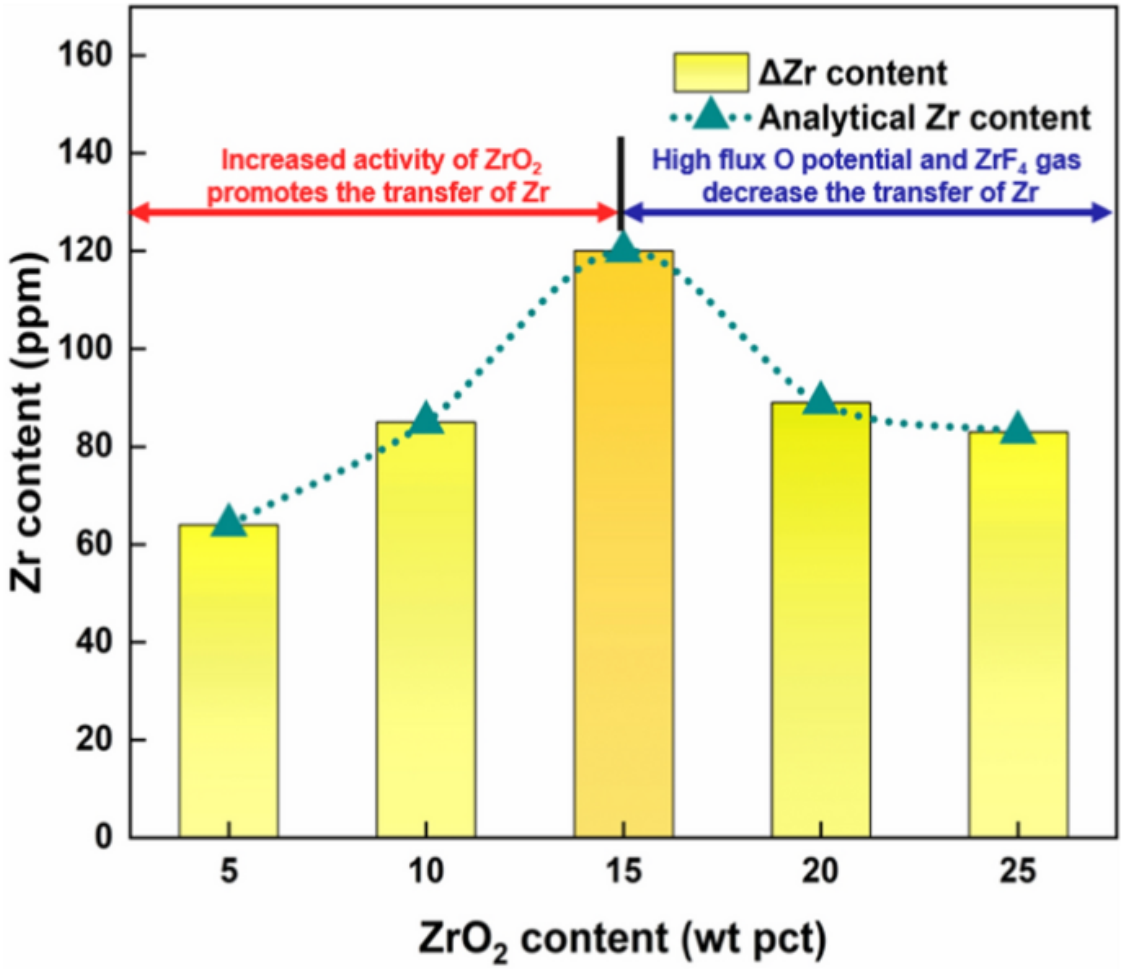

Fig. 4. Variation of Zr content as a function of ZrO_2 content in the flux

It is illustrated in Figure 4 that ΔZr value increases from 64 to 120 ppm with the addition of ZrO_2 from 5 to 15 wt pct, and then reduces to 85 ppm with further addition up to 25 wt pct. Initially, the increased activity of ZrO_2 in the flux from 0.07 to 0.20 (as shown in Figure 1) promotes the transfer of Zr to the weld pool. However, with additions higher than 15 wt pct, the increased flux O potential suppresses the transfer of Zr, which is similar to the conclusion raised by Zhang *et al*.[24] Furthermore, the presence of ZrF_4 in the gaseous phase (as shown in Table V of Appendix A) illustrates the chemical interaction between CaF_2 and ZrO_2, which may promote the reduction of Zr to the gaseous phase. Calculated by FactSage 7.3, the increment of ZrF_4 gas reaches up to 22.6 vol pct with ZrO_2 addition ranging from 15 to 25 wt pct, which is approximately 5 times compared with the increment of ZrF_4 gas when the ZrO_2 addition varies from 5 to 15 wt pct. Such a phenomenon reveals the evident increased loss of Zr to the gaseous phase in the form of ZrF_4 when the ZrO_2 content is higher than 15 wt pct. Meanwhile, it is calculated by FactSage 7.3 that the quantity of Zr that exists in the gaseous phase increases from 0.013 to 0.30 with the addition of ZrO_2 from 5 to 25 wt pct, which in turn demonstrated that the decreased transfer of Zr to the WM with increased ZrO_2 addition is due to the Zr lost to the gaseous phase.

Electrochemical reactions could be another factor that determines the transfer of O and Zr when direct current is applied during the SAW process.[22] Frost *et al*.[27] demonstrated that the existence of electrochemical reactions at the anode might change the transfer quantity of O. Coetsee *et al*.[18] further pointed out that O^{2-} could be recovered to form O under the arc plasma.

As shown in Figure 5, electrochemical Reactions [6] and [7] occurring at the anode may likely influence the transfer of O. The increased ZrO_2 content promotes the release of O^{2-} in the arc plasma *via* Reaction [6] due to oxide dissociation at the high temperature inherent from the arc cavity. Then, increased ZrO_2 enhances the quantity of O transferred from the slag to the WM *via* the arc plasma as displayed in Reaction [7].[18,25] Furthermore, it is proven by Forst and Olson *et al*.[15,27] that the electrochemical reduction reaction could occur at the cathode (weld pool) and assist the transfer of alloying elements from the arc plasma to the weld pool. In this study, the increased ZrO_2 activity with increased addition of ZrO_2 further promotes the decomposition of ZrO_2 in the arc plasma, leading to a higher Zr^{2+} concentration *via* Reaction [6], which increases the transfer of Zr through Reaction [8] occurring at the cathode (weld pool).[27,28]

$$\mathrm{ZrO\ (g) = Zr^{2+}\ (plasma) + O^{2-}\ (plasma)}, \tag{6}$$

$$\mathrm{O^{2-}\ (plasma) = [O] + 2e^{-}}, \tag{7}$$

$$\mathrm{Zr^{2+}\ (plasma) + 2e^{-} = [Zr]}. \tag{8}$$

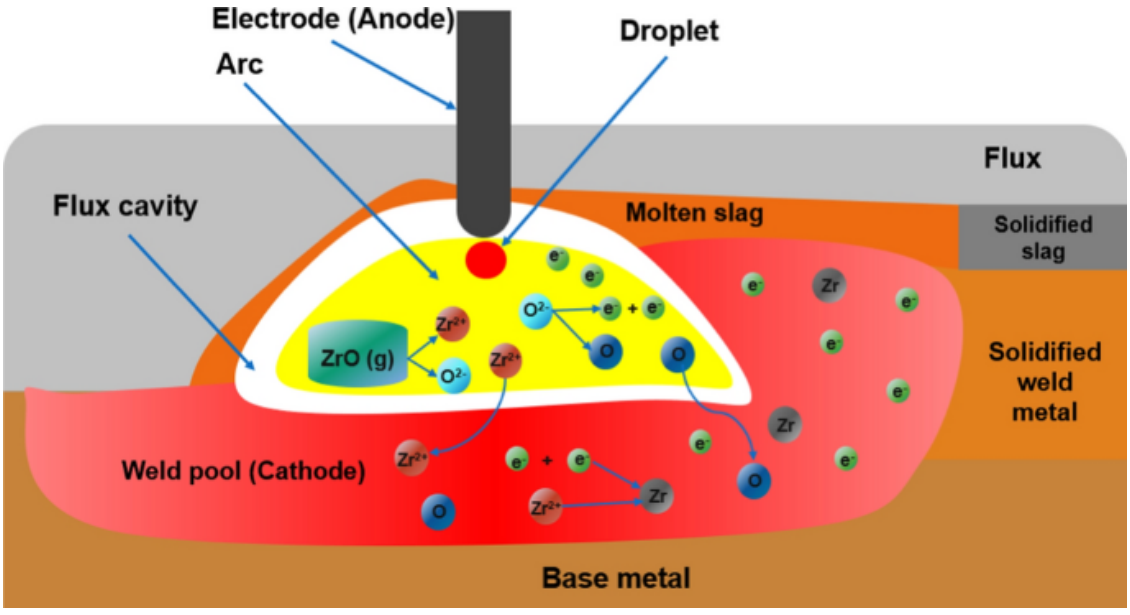

Fig. 5. Schematic diagram of the electrochemical reactions during SAW

Figure 6 shows the ΔSi value increases from −0.062 to −0.018 wt pct with ZrO_2 addition ranging from 5 to 25 wt pct when the SiO_2 content of each flux remains at approximately 6.8 wt pct. This phenomenon implies that an increased quantity of Si was oxidized and lost to the slag due to the presence of O in the weld pool.[24,25] It is further demonstrated that the

transferred quantity of Si was mainly controlled by SiO_2 decomposition *via* Reaction [9].[29,30] Meanwhile, δSiO_2 value slightly increases from −0.17 to −0.02 as the ZrO_2 content varies from 5 to 25 wt pct. It can be seen that both the slag and the weld pool lose Si during SAW. Therefore, according to the mass conservation law, it is postulated that Si is transferred to the gaseous phase in the form of SiF_4.[31,32] To further study the variation of SiF_4 with different ZrO_2 contents, calculation results by FactSage 7.3 as displayed in Table IV show that the content of SiF_4 increases from 0.025 to 0.19 vol pct with ZrO_2 addition ranging from 5 to 25 wt pct, which in turn reveals the increased loss of Si to the gaseous phase.

$$(SiO_2) = [Si] + 2[O]. \quad (9)$$

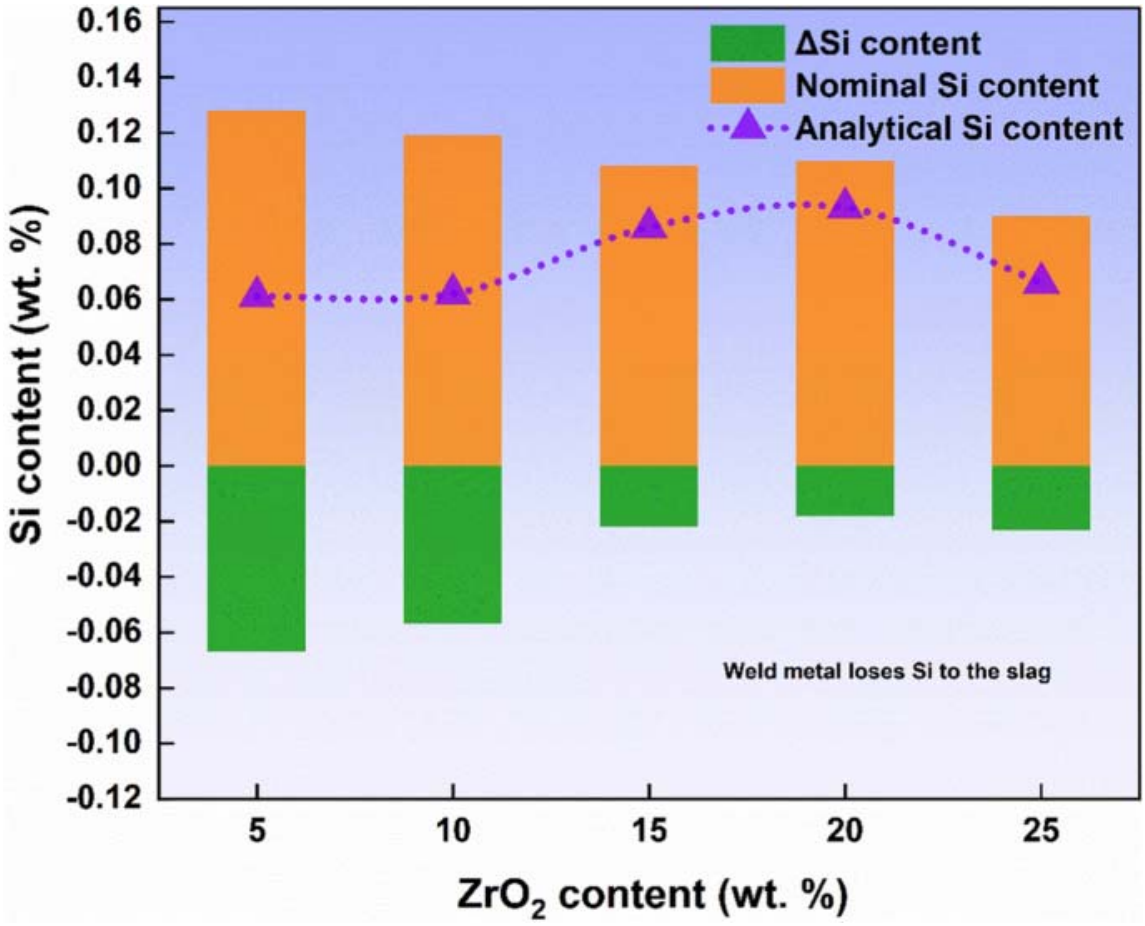

Fig. 6. Variation of Si as a function of ZrO_2 content in the flux

Table IV. SiF_4 Gas Content of Each Flux Composition (Vol Pct)

Fluxes No.	F-1	F-2	F-3	F-4	F-5
SiF_4	2.5×10^{-2}	2.7×10^{-2}	2.2×10^{-2}	6.4×10^{-2}	0.19

In this study, the role of ZrO_2 in major alloying element transfer behaviors has been investigated from thermodynamic and electrochemical perspectives. The superior O supply

capacity of ZrO_2 reflects its excellent decomposability during the SAW process. In addition, the maximum transfer of Zr could reach up to 120 ppm, but it tends to be suppressed due to the high oxygen potential of the flux and is lost to the gaseous phase in the form of ZrF_4 when the ZrO_2 content of the flux is higher than 15 wt pct.[18] Considering ZrF_4 gas is formed by chemical interaction between CaF_2 and ZrO_2, the design of ZrO_2-bearing fluxes needs to reduce fluoride content to enhance the transfer of Zr.

Conclusions

In summary, five CaF_2-ZrO_2-agglomerated fluxes with varying ZrO_2 additions have been designed to weld EH36-shipbuilding steel under 60 kJ/cm heat input to study the transfer behavior of main alloying elements. The conclusions of this study are as follows:

1. The increased ZrO_2 activity and the anode electrochemical reaction promote the transfer of O from 190 to 370 ppm with ZrO_2 content ranging from 5 to 25 wt pct. ZrO_2, compared with SiO_2 and MnO, possesses a higher O supply capacity during SAW.
2. The transfer of Zr reaches to the maximum value of 120 ppm when the ZrO_2 content of the flux is 15 wt pct. Formation of ZrF_4 and SiF_4 gas causes the loss of Zr and Si to the gaseous phase and further decreases the transfer of Zr and Si to the WM, respectively.

Acknowledgments

The authors sincerely acknowledge the financial support from the National Key R&D Program of China (Grant Nos. 2023YFB3709900, 2023YFB3709902, and 2022YFE0123300), the National Natural Science Foundation of China (Grant Nos. U20A20277 and 52350610266), the Fundamental Research Funds for the Central Universities (Grant No. N2402016), and the Major Project of Liaoning Province Innovation Consortium (Grant No. 2023JH1/11200012).

Conflict of interest

On behalf of all authors, the corresponding author states that there is no conflict of interest.

References

1. Y. Zhang, J. Yang, D. Liu, X. Pan, and L. Xu: *Metall. Mater. Trans. A*, 2021, vol. 52A, pp. 668–79.
2. R. Sakamoto, K. Kobayashi, T. Iijima, and Y. Mizo: *Weld. World*, 2012, vol. 56, pp. 64–71.
3. C. Wang and J. Zhang: *Acta Metall. Sin.*, 2021, vol. 57, pp. 1126–40.
4. J. Zhang, C. Wang, and T. Coetsee: *Metall. Mater. Trans. B*, 2021, vol. 52B, pp. 1937–44.
5. P. Layus, P. Kah, and V. Gezha: *J. Eng. Mech.*, 2018, vol. 232, pp. 114–27.
6. L. Sun, Z. Xu, L. Peng, and X. Lai: *J. Scr. Mater.*, 2022, vol. 219, p. 114877.
7. N. Fujiyama and G. Shigesato: *ISIJ Int.*, 2021, vol. 61, pp. 1614–22.
8. D. Loder, S.K. Michelic, and C. Bernhard: *J. Mater. Sci. Res*, 2017, vol. 6, pp. 24–43.
9. J. Dowling, J. Corbett, and H. Kerr: *Metall. Mater. Trans. A*, 1986, vol. 17A, pp. 1611–23.
10. S. Kou: *Welding metallurgy*, 2nd ed. Wiley, New York, 2003, pp. 22–95.

11. C. Chai and T. Eagar: *Weld. J.*, 1982, vol. 61, pp. 229–32.
12. Y. Zhang, H. Liu, T. Coetsee, Z. Wang, and C. Wang: *Metall. Mater. Trans. B*, 2023, vol. 54B, pp. 2875–80.
13. X. Zou, J. Sun, D. Zhao, H. Matsuura, and C. Wang: *J. Iron. Steel Res. Int.*, 2018, vol. 25, pp. 164–72.
14. S. Kurlanov, N. Potapov, and O. Natapov: *Weld. Int.*, 1993, vol. 7, pp. 65–68.
15. C. Natalie, D. Olson, and M. Blander: *Annu. Rev. Mater. Sci.*, 1986, vol. 16, pp. 389–413.
16. N. Potapov and S. Kurlanov: *Weld. Int.*, 1987, vol. 1, pp. 951–54.
17. K. Bang, C. Park, H. Jung, and J. Lee: *Met. Mater. Int.*, 2009, vol. 15, pp. 471–77.
18. T. Coetsee and F. De Bruin: *Processes*, 2023, vol. 11, p. 658.
19. P. Kanjilal, S. Majumdar, and T. Pal: *ISIJ Int.*, 2005, vol. 45, pp. 876–85.
20. V. Sengupta, D. Havrylov, and P. Mendez: *Weld. J.*, 2019, vol. 98, pp. 283–313.
21. J.H. Park: *Calphad*, 2007, vol. 31, pp. 149–54.
22. T. Coetsee, R. Mostert, P.G.H. Pistorius, and P.C. Pistorius: *J. Mater. Res. Technol*, 2021, vol. 11, pp. 2021–2036.
23. C. Chai and T. Eagar: *Metall. Trans. B*, 1981, vol. 12B, pp. 539–47.
24. J. Zhang, T. Coetsee, H. Dong, and C. Wang: *Metall. Mater. Trans. B*, 2020, vol. 51B, pp. 1953–57.
25. T. Coetsee and F. De Bruin: *Processes*, 2021, vol. 9, p. 1763.
26. J. Zhang, T. Coetsee, S. Basu, and C. Wang: *Calphad*, 2020, vol. 71, p. 102195.
27. J. Kim, R. Frost, D. Olson, and M. Blander: *Weld. J.*, 1990, vol. 69, pp. 446–53.
28. J. Pu, S. Yu, and Y. Li: *J. Alloys Compd.*, 2017, vol. 692, pp. 351–58.
29. J. Zhang, T. Coetsee, H. Dong, and C. Wang: *Metall. Mater. Trans. B*, 2020, vol. 51A, pp. 1350–54.
30. J. Kim, T. Lee, and I. Sohn: *Metall. Mater. Trans. A*, 2018, vol. 49A, pp. 2705–20.
31. T. Lau, G. Weatherly, and A. Mclean: *Weld. J.*, 1986, vol. 65, pp. 343–47.
32. J. Du Plessis, M. Du Toit, and P. Pistorius: *Weld. J.*, 2007, vol. 86, pp. 273–80.

Appendix A: Thermodynamic Calculation

Thermodynamic calculations were conducted using FactSage 7.3. The Equilib Module was selected, and the gas–slag–metal equilibrium model was applied.[18] FToxid, FSstel, and FactPS databases were selected due to the presence of oxides, liquid metal, and gas during submerged arc welding (SAW). The equilibrium temperature of 2273 K was applied. The mass ratio of flux, base metal (BM), and wire were set as unity, in accordance with a previous study.[18] Relevant data for the main components in the slag, liquid, and gas phases when 5 wt pct ZrO_2 is added to the flux are illustrated in Table V.

Table V. Equlibrium Slag, Liquid, and Gaseous Phases Compositions

Slag Phase (Wt Pct)	Liquid Phase (Wt Pct)	Gaseous Phase (Vol Pct)
CaF_2 51.88	Zr 0.08	CaF_2 86.17
ZrO_2 5.44	Fe 97.19	Na 4.50
SiO_2 1.18	Mn 0.79	CO 1.00
Na_2O 0.01	Si 1.90	SiF_4 2.5×10^{-2}
FeO 5.53	C 0.09	ZrF_4 1.0
MnO 0.63	O 1.20×10^{-3}	O_2 2.11×10^{-10}
CaO 14.22	Ni 0.01	ZrO 9.15×10^{-7}